Structural Integrity Issues from Crack Nucleation, Initiation and Growth

Xijia Wu and Zhong Zhang
Aerospace Research Center, National Research Council Canada
1200 Montreal Road, Ottawa, ON
CANADA

Xijia.Wu@nrc-cnrc.gc.ca

Keywords: Fatigue, crack nucleation, crack initiation, crack growth, structural integrity, total life.

ABSTRACT

In this article, some key aspects of fatigue crack nucleation and growth are discussed with an emphasis on total fatigue life prediction. Recently, it has been shown that fatigue crack nucleation life can be analytically predicted with the TMW model knowing the material's elastic modulus, Poisson's ration, Burgers vector, surface energy, the surface roughness, and the applied plastic strain range, without resorting to fatigue testing. This advance is very important as crack nucleation takes a significant portion of the total life in structural integrity. The same model is extended for crack nucleation in terms of mean root square of plastic strain or stress amplitudes under variable amplitude loading. In addition, a total life analysis example is given for the key-hole specimens using the TMW model and the Paris law.

1.0 INTRODUCTION

The study of structural integrity has been a continuing effort since Wöhler first conducted fatigue tests to establish S-N relations for railway steels in the 1860s [1]. Accurate assessment of the holistic life from crack initiation and growth to failure is even more important as the integrated vehicle health management (IVHM) is used to modernize life cycle management. In this scheme, the damage state of the structure and its remaining structural integrity needs to be known continuously at any time in service, in order to optimize mission and maintenance planning to increase availability and avoid unexpected failure. Traditionally, two distinct lifing approaches are pursued for structural design: "safe life" and "damage-tolerance". In the continuum sense, *Safe Life* assumes that no cracks would exist in the structure during the specified lifetime for safe operation, and the component must be removed from service at the end of the "safe life". Nowadays, the "safe life" is equivalent to the crack initiation life, but there is no uniform definition for the crack initiation size. Thus, it leaves a gap between physical crack initiation and detectable cracks within the structure. The *Damage Tolerance* approach is quantified as a structural ability to endure the growth of cracks from detectable initial flaws to fracture. The missing description for crack growth ranges from a few microns to a few millimetres, which is classified as the small crack growth stage, where the crack mechanics has not been well-defined (or, at least, commonly agreed to within the engineering community). This makes the total structural life dependent on the definition of "crack initiation". Therefore, for IVHM, there is a strong need to predict the total life of the structure with the presence of cracks for structural integrity updates.

It has long been recognized that fatigue crack propagation in metals exhibits two consecutive modes: a crystallographic shear mode (Stage I) followed by a non-crystallographic tensile mode (Stage II) [2, 3], as schematically shown in Figure 1. After the fatigue crack nucleates from persistent slip bands (PSB) in stage I, it propagates as a result of co-planar alternating slips. In stage II, crack propagation is associated with wavy slip along multiple slip systems such that the main crack path is almost perpendicular to the principal load axis. Thus, the holistic fatigue damage process, called the holistic structural integrity process (HOLSIP) [4], is divided into four categories: i) crack nucleation, ii) small crack growth, iii) long crack growth, and iv) unstable crack growth to failure. This division is mainly based on the mechanistic argument (continuum mechanics, linear elastic or elastoplastic fracture mechanics) applicable to the particular category. However,

questions remain on the crack size range where the theory is valid. Thus, a holistic life prediction methodology should be developed to provide a stage-by-stage structural integrity management strategy, which can be combined with in-situ health monitoring, to provide a more accurate and efficient approach for extended operations as well as increased repair limits.

This paper will first introduce the Tanaka-Mura-Wu (TMW) model for crack nucleation under constant amplitude loading, and then extend it to variable amplitude loading cases. Then, examples of total life treatments are given, combining the TMW crack initiation model with fracture mechanics treatment of crack growth (Paris equation), to demonstrate an expedient method of fatigue life prediction. The current treatment only focuses on fatigue of metallic materials in an ambient environment. High temperature and aggressive environment will induce more complications, which can be tackled following a mechanism-based modelling approach via the integrated creep-fatigue theory (ICFT) [5].

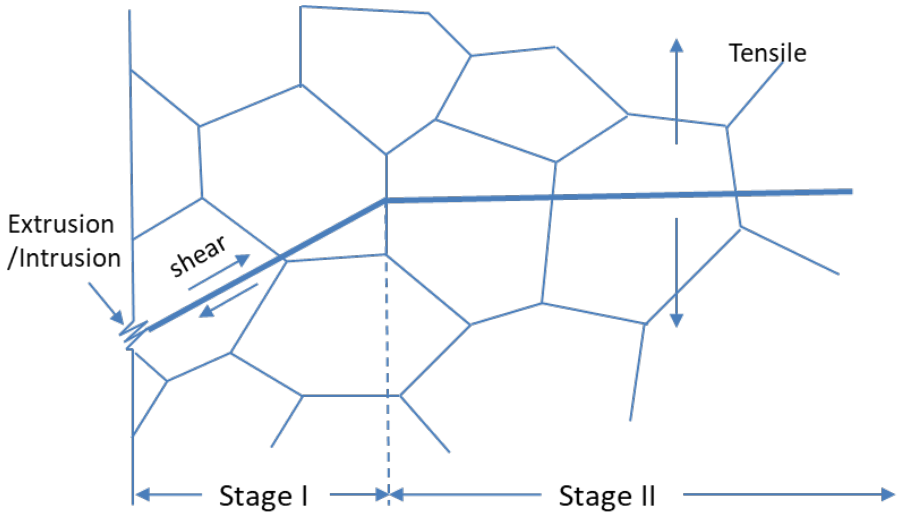

Figure 1. Schematic of fatigue crack nucleation and propagation in polycrystalline metals.

2.0 MODELLING CRACK NUCLEATION/INITIATION

In the literature, crack nucleation and crack initiation are both used to refer to the occurrence of cracking. For the sake of structural integrity, the two concepts need to be clarified. It is understood that crack nucleation refers to the process leading to the very first instance of crack formation; while crack initiation means the appearance of a crack that can be found with a definite size. For example, the United States Air Force (USAF) regards the crack initiation size to be 0.05 inch (1.27 mm); whereas the US Navy (USN) defines a crack as having been initiated when it is “0.01 inch-long” (0.254 mm), based on its detectability [6]. The definition of crack initiation with a pre-defined size provides a division point for engineering design, below which continuum-based safe life methodologies apply and above which fracture mechanics methodologies apply. However, such crack initiation definitions are not from the physics of failure but imposed based on detectability. This introduces a period of ambiguous crack existence in characterizing the holistic structural integrity.

2.1 Fatigue Crack Nucleation under Constant Amplitude Loading

The fatigue crack nucleation process has been understood to start with formation of persistent slip bands (PSBs) under cyclic loading [7]. Dislocations emanating from PSBs can form intrusions and extrusions on

the surface. Extrusions can be regarded as interstitial dipoles left at the surface, while intrusions consists of vacancy dipoles [8], as schematically shown in Figure 2. Many metallurgical observations have been made on crack nucleation at PSBs [9, 10]. A fatigue crack nucleation model was originally envisaged by Tanaka and Mura, based on continuously-distributed inverted dislocation pileup [11]. Recently, the plastic shear strain γ of the dislocation pileup has been revised by Wu, removing the physical dimension of [m^2], to be expressed as [12]:

$$\Delta\gamma = \frac{2(1-v)(\Delta\tau - 2k)}{\mu} \qquad (1)$$

where τ is the applied shear stress, k is the lattice resistance on the slip system, μ is the shear modulus, *v* is Poisson's ratio, *b* is the Burgers vector.

The dislocation pile-up energy accumulated each cycle is given by

$$\Delta U = \frac{1}{2}(\Delta\tau - 2k)\Delta\gamma \qquad (2)$$

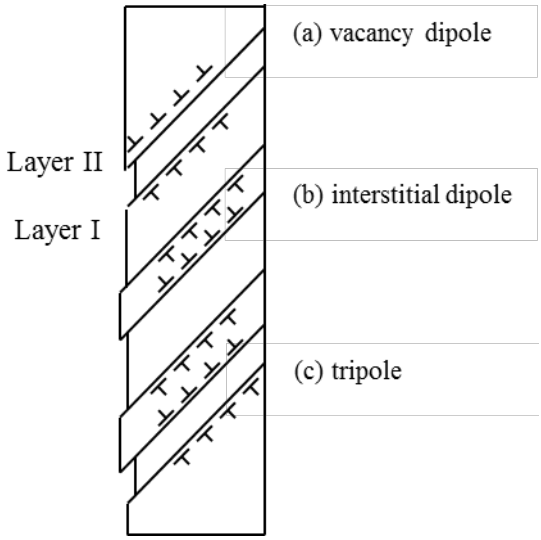

Figure 2. Dislocations in (a) vacancy dipoles (forming an intrusion), (b) interstitial dipoles (forming an extrusion) and (c) tripoles (forming an intrusion-extrusion pair) at the surface.

Fatigue crack nucleation happens under constant amplitude loading when the total accumulated energy is equal to the energy of forming new crack surfaces of 2*a* (the Griffith criterion):

$$N\Delta Uba = 2w_s a \qquad (3)$$

where *a* is the crack nucleation size (dislocation pileup distribution length) and w_s is the surface energy, J/m^2.

Then, the cycle to crack nucleation can be obtained, by substituting Eq. (1)-(2) into Eq. (3), as [12]

$$N_c = \frac{8(1-\nu)w_s}{\mu b}\frac{1}{\Delta\gamma^2} \tag{4}$$

or, in terms of stress,

$$N_c = \frac{2\mu w_s}{(1-\nu)(\Delta\tau - 2k)^2 b} \tag{5}$$

In engineering practice, fatigue life is assessed through testing of material coupons with a prescribed surface finish achieved through machining. Therefore, we need to introduce a surface roughness factor R_s, to account for its effect in nominal machining conditions. Using the Taylor factor relationship $\gamma = \sqrt{3}\varepsilon$ and $\tau = \sigma/\sqrt{3}$, Eq. (4) and (5) can be converted into

$$N_c = \frac{8(1-\nu)R_s w_s}{3\mu b}\frac{1}{\Delta\varepsilon_p^2} \tag{6}$$

and

$$N_c = \frac{6\mu w_s}{(1-\nu)(\Delta\sigma - 2\sigma_0)^2 b} \tag{7}$$

Here it is assumed that surface roughness would directly enhance intrusion/extrusion associated with cyclic plasticity, but its effect on intrusion/extrusion is ignored with elastic deformation, so $R_s = 1$ below the yield stress, but its effect may be manifested in σ_0 to a certain extent.

The strain-based formula, Eq. (6), has been validated for Type 316 stainless steel, copper, titanium, tungsten, Waspaloy and Mar-M 509, just based on the materials' known physical properties, w_s, μ, ν, and b [12]. The materials' surface energies can be found from Tyson and Miller's work [13], where $w_s = w_s(T_m) + \phi(T)\frac{RT_m}{A}$, $w_s(T_m)$ is the surface energy at the melting temperature T_m, RT_m/A (R is the universal gas constant, A is the surface area per molar atoms), the value of both terms are given in [13]; $\phi(T)$ is an entropy related term which takes values from 0 at melting point and 1 at absolute zero temperature. It is approximately ~0.85 at ambient temperature. Figure 3 shows the low cycle fatigue (LCF) lives of Type 316 stainless steel with different surface finishes. The theoretical prediction of Eq. (6) exactly matches the experimental data for the electropolished surface obtained from Wareing and Vaughan [14] with $R^2 = 0.986$, which represents an "ideal" case. By comparison, the machined surface roughness has an effect of $R_s \sim 1/3$, with $R^2 = 0.976$.

The room-temperature uniaxial LCF life vs. plastic strain relations of several metals and alloys including Type 316 stainless steel [14], copper [15], titanium [16], tungsten [17], Waspaloy [18], and Mar-M 509 [19] are shown in Figure 4, also in comparison with Eq. (6) with surface roughness factor $R_s = 1/3$ (assuming the same machined condition). The material properties and the calculated values of the fatigue life coefficient are given in Table 1, with all materials being assumed to have a Poisson's ratio of 0.3. The theoretical predictions of Eq. (6) are in very good agreement with experimental data with a scatter factor of 2 in the LCF range ($< 10^4$), as shown in Figure 4, even for Waspaloy with different grain sizes (125 μm, coarse grained (CG); 16 μm, fine grained (FG)). Towards HCF with $\varepsilon_p < 10^{-4}$, the scatter becomes larger as microstructural inhomogeneity effect becomes stronger. As materials with high surface energy often have a high elastic modulus and high melting temperature, the LCF life behaviour seems to be unified by the w_s/μ ratio. In terms of stress, however, the microstructure can have a more pronounced effect, since the grain boundaries and precipitates may affect the lattice friction resistance k (e.g., via the Hall-Petch relationship or Orowan looping formula) in Eq. (5) and (7). Also, in alloys, solute atoms may have an effect on the surface energy, as compared to pure metals.

Fatigue life behaviours are often described with an empirical correlation—Coffin-Manson and Basquin

(CMB) relation [20, 21, 22]:

$$\frac{\Delta\varepsilon}{2} = \frac{\sigma'_f}{E}(2N)^b + \varepsilon'_f(2N)^c \qquad (8)$$

where σ'_f, ε'_f, b, c are empirical constants.

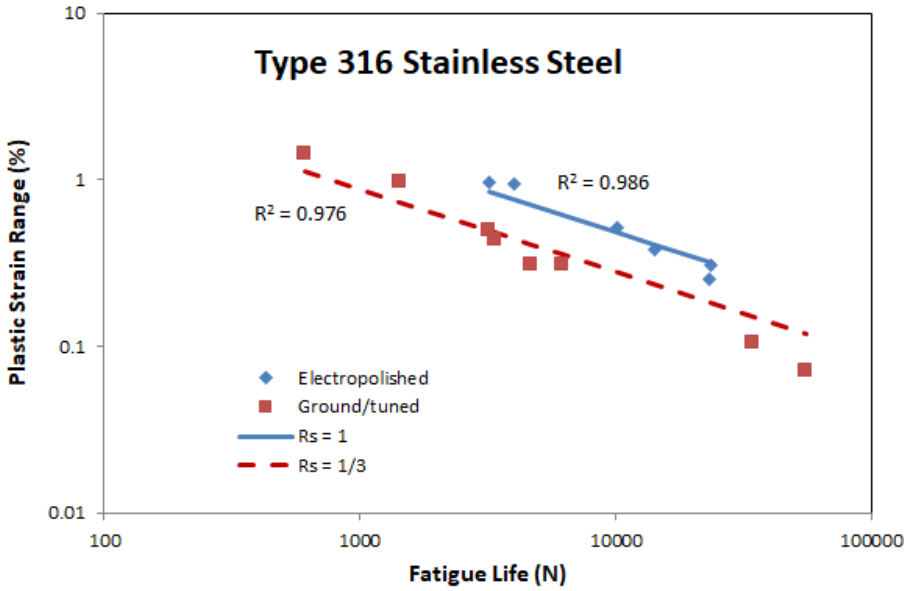

Figure 3. Fatigue life of Type 316 stainless steel with different surface finish. The symbols represent the experimental data taken from [14]. The lines represent theoretical predictions of Eq. (6).

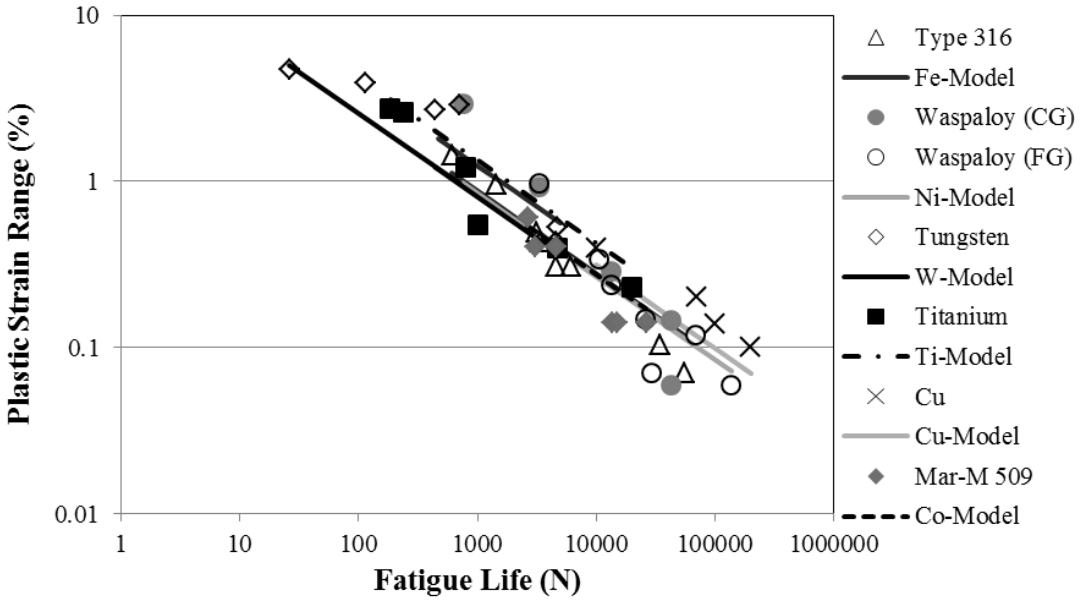

Figure 4. Predicted fatigue curves in comparison with experimental data.

Table 1. Fatigue Coefficients in Eq. (6) for a Number of Metals/Alloys

Material	E (GPa)	b (10^{-10} m)	$\frac{8(1-\nu)R_s w_s}{3\mu b}$
Cu	112	2.56	0.099
Ti	54.5	3.21	0.181
W	286	2.74	0.066
Fe (Type 316 SS)	199	2.48	0.117
Ni (Waspaloy)	211	2.48	0.072
Co (Mar-M 509)	211	2.48	0.077
Al (7075-T6)	71	2.86	0.090

Eq. (8) relies on a large amount of fatigue test data for regression analysis to determine the empirical constants. For material development and structural design, fatigue testing has been a significant cost factor in terms of both time and money. It will be a huge advantage if fatigue properties of materials could be accurately estimated analytically, especially for new materials. To demonstrate the feasibility of this approach, the Tanaka-Mura-Wu (TMW) model, Eq. (6), is used to describe the LCF life of several alloys with the Ramberg-Osgood equation representing the cyclic stress-strain relationship:

$$\frac{\Delta\varepsilon}{2}=\frac{\Delta\sigma}{2E}+\left(\frac{\Delta\sigma}{2K'}\right)^{\frac{1}{n'}} \qquad (9)$$

where *K'* is the cyclic plastic strength, and *n' is* the strain sensitivity.

The first example is 7075-T6, which is an age-hardenable aluminium alloy with peak strength at the T6 temper. The alloy is widely used in aerospace applications, owing to its high specific strength, toughness, good ductility and fatigue resistance. The prediction of Eq. (6) using the parameters of Al (Table 1) for 7075-T6 is shown in Figure 5 in comparison with the CMB relation. The Ramberg-Osgood equation and CMB equation parameters for 7075-T6 are taken from [23] and given in Table 2, from which the plastic strain range is calculated and substituted into Eq. (6) to compute the fatigue life. Excellent agreement is found between the TMW model prediction and the description of CMB equation but without fitting. In addition, two automotive steels: Men-Ten and RQC-100 steels are studied. The two materials were used in a test program conducted by the Society of Automotive Engineers (SAE) Fatigue Design & Evaluation Committee to provide a set of basic data for determining the validity of various fatigue life estimation and analysis methods [24]. The Ramberg-Osgood and CMB relation parameters for these materials are taken from [24] and also given in Table 2. The predictions of Eq. (6) using the properties of Fe (Table 1) and plastic strain range evaluated from the Ramberg-Osgood relations for Men-Ten and RQC-100 are shown in Figure 6 and 7, respectively. Again, excellent agreements are found between the TMW model prediction and the CMB equation. It should be noted that towards the fatigue limit, the accuracy of prediction using the strain-based Eq. (6) will depend on how well the Ramberg-Osgood equation represents the material's cyclic stress-strain

response. It is advised that Eq. (7) be used near the fatigue endurance limit with calibration, as discussed elsewhere [25].

Table 2. Empirical Parameters for Material Cyclic Properties

Material	K' (MPa)	n'	σ_f' (MPa)	b	ε_f'	c
7075-T6	780.64	0.088	780.64	-0.045	0.19	-0.52
Men-Ten	1200.6	0.02	915	-0.095	0.26	-0.47
RQC-100	1131.6	0.01	1160	-0.075	1.26	-0.75

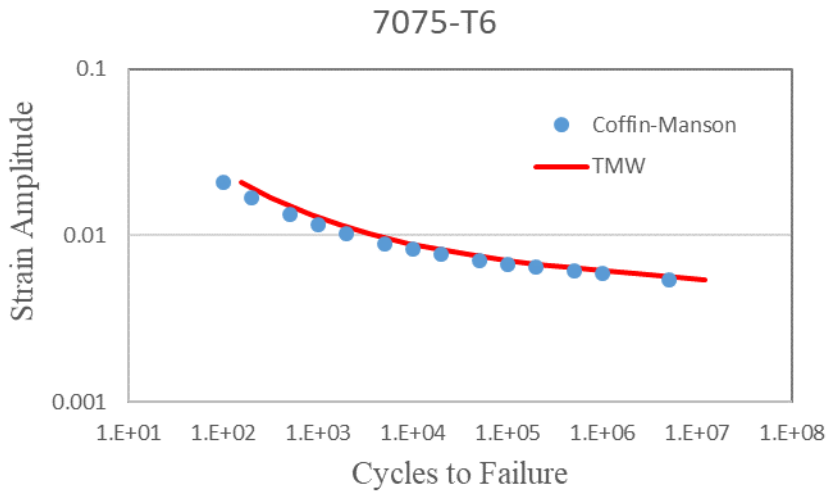

Figure 5. Theoretical prediction of Eq. (6) in comparison with Coffin-Manson-Basquin curve for Al 7075-T6.

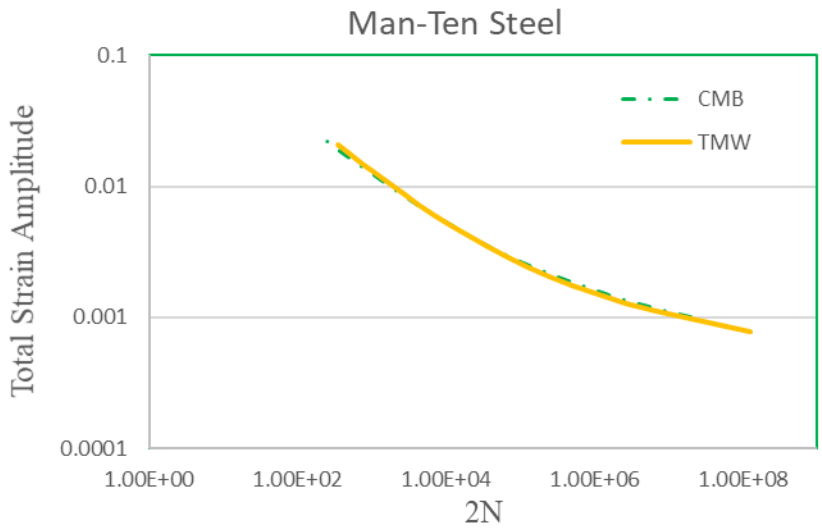

Figure 6. Theoretical prediction of Eq. (15) in comparison with Coffin-Manson-Basquin curve for

Men-Ten steel.

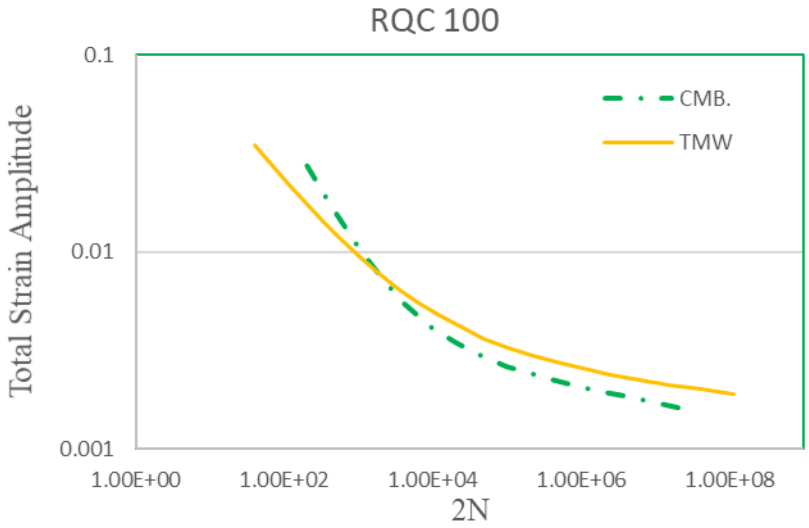

Figure 7. Theoretical prediction of Eq. (6) in comparison with Coffin-Manson-Basquin curve for RQC-100 steel.

2.2 Fatigue Crack Nucleation under Variable Amplitude Loading

Engineering components/structures such as airframes, landing gears, and gas turbine engine components in service often experience variable loading. Palmgren and Miner introduced a linear summation rule [26, 27], as:

$$\sum_i \frac{N_i}{N_{fi}} = 1 \qquad (10)$$

where N_i is the number of load cycles and N_{fi} is the fatigue life at the i-th load level.

Based on the energy consideration, the TMW model can be extended to variable amplitude loading conditions as follows.

Under variable amplitude loading, the dislocation dipole pile-up energy accumulated will be:

$$\sum_i^N \Delta U_i ba = 2w_s a \qquad (11)$$

where ΔU_i is the strain energy at the i-th load level.

Then, substituting Eq. (1) and (2) for the i-th load level into (11), we obtain:

$$\sum_i^N \Delta\gamma_i^2 = \frac{8(1-v)w_s}{\mu b} \qquad (12)$$

Similarly, in terms of stress ranges:

$$\sum_{i}^{N}(\Delta\tau_i - 2k)^2 = \frac{2\mu w_s}{(1-v)b} \qquad (13)$$

It can be proven that both Eq. (12) and Eq. (13) can turn into the Palmgren-Miner rule, Eq. (10), by dividing the right-hand terms and equating N_{fi} to N_c in Eq. (4) and (5). As it is based on energy consumption, both strain-based and stress-based formula can be mixed in the above summation, depending on whether the load range is in the elastic or plastic regime. Furthermore, if we define the root mean square (RMS) of load ranges as:

$$\Delta\gamma_{RMS} = \sqrt{\frac{1}{N}\sum_{i}^{N}\Delta\gamma_i^2} \qquad (14)$$

$$(\Delta\tau - 2k)_{RMS} = \sqrt{\frac{1}{N}\sum_{i}^{N}(\Delta\tau_i - 2k)^2} \qquad (15)$$

Eq. (12) and (13) become

$$N_c = \frac{8(1-v)w_s}{\mu b}\frac{1}{{\Delta\gamma_{RMS}}^2} \qquad (16)$$

and

$$N_c = \frac{2\mu w_s}{(1-v)b{(\Delta\tau - 2k)_{RMS}}^2} \qquad (17)$$

Eq. (16) and (17) have the same form as Eq. (4) and (5), except using the root mean square of the variable load range to replace the constant amplitude load range. These equations offer a great expedient method of estimating the variable-amplitude fatigue life in terms of the RMS for a loading profile, instead of conducting fatigue testing at each load level and summing up the ratio of fatigue lives. Here, we take Aid et al.'s experimental results on 6082-T6 aluminium alloy [28] for illustration. Variable amplitude fatigue tests were conducted using four blocks of different stress amplitudes in Low-to-High, High-to-Low, and Random sequential orders. The experimental results of constant amplitude fatigue at each load level, the block cycle number, and sequence order (from 1 to 4) are given in Table 3. From the loading profile, it is easy to calculate the RMS, then Eq. (17) is used to calculate the total cycle life, where $(\Delta\tau - 2k)$ is replaced with $2(\sigma_{max} - \sigma_0)/\sqrt{3}$, E = 71 GPa, w_s = 1.12 J/m^2 at room temperature, b = 2.86×10^{-10}m, and σ_0 = 220 MPa is considered as the fatigue limit. It can be seen in Table 3 that the predicted total cycle is very close to the experimental observation.

Table 3. Variable Amplitude Fatigue of Al6082-T6

Block #	Nf	Smax(MPa	Block-Seq	Ni	Block-Seq	Ni	Block-Seq	Ni
1	394765	240	1	103000	4	52500	4	43400
2	180660	260	2	26258	3	26258	3	26258
3	87612	280	3	19427	2	19427	1	19427
4	38000	305	4	16800	1	10950	2	10950
		RMS	Total	165485	Total	109135	Total	100035
			Predicted	138627	Predicted	118352	Predicted	110378

3.0 HOLISTIC STRCTURAL LIFE PREDICTION

With the exception of crack initiation life, with its varying crack size definition, fatigue crack growth has also been studied extensively with various issues such as fatigue threshold and crack closure [29-71]. Fatigue crack growth problems are often divided into i) short-crack growth and ii) long-crack growth problems. Short cracks may also be classified into several categories: *mechanically-short cracks, microstructurally-short cracks, physically-short cracks,* and *chemically short cracks,* ranging from a few microns to a few millimetres [29], while the long-crack growth behaviour is well described in terms of the linear elastic fracture mechanics (LEFM) parameter—the stress intensity factor—*K*, as given by the Paris equation [54]:

$$\frac{da}{dN} = C(\Delta K)^n \tag{18}$$

where C and n are empirical constants.

The long-crack behaviour is more deterministic, whereas the short-crack behaviour is probabilistic [38, 39] as it is affected by the local microstructural constraints in materials comprised of randomly orientated grains. Relative to artifically prepared cracks (precracking), the behaviour of naturally initiated cracks is much less studied. Acturally, monitoring the growth of naturally initiated cracks is crucial in structural health management (SHM), which is now emphasized for structural integrity prognosis. Natural crack initiation and growth are a part of the holisitc structural integrity process (HOLSIP), for which efficient engineering methods should be developed to meet the SHM demands.

In the 1970's, the Society of Automotive Engineers (SAE) Fatigue Design & Evaluation Committee conducted a test program to provide a set of basic data for determining the validity of various fatigue life estimation and analysis methods, using a key-hole specimen, incorporating two steels commonly used in the ground vehicle industry. Both constant amplitude and variable amplitude tests were performed on the "key-hole" specimen. Details of the test program can be found on the eFatigue website: (https://www.efatigue.com/benchmarks/SAE_keyhole/SAE_keyhole.html). In this section, the SAE key hole problem is re-analyzed to demonstrate the HOLSIP approach with the TMW model and the Paris equation.

The present case-study concerns the total fatigue life of the key–hole specimen made of RQC-100 steel under constant amplitude loading of 13.3 kN, R = -1 (i.e., the test case CR-1). First, an elastic stress analysis was conducted using MSC.Marc and the stress-contours are shown in Figure 8a. The maximum stress is found to be 458 MPa at the notch root of the key-hole. Based on Molski and Glinka's approach [72]—a modification of Neuber's rule with the Ramberg-Osgood relationship, the notch root stress is found to satisfy:

$$\frac{(\sigma_{max})^2}{2E} = \frac{\sigma_a^2}{2E} + \frac{\sigma_a}{n+1}\left(\frac{\sigma_a}{K}\right)^{\frac{1}{n}} \qquad (19)$$

where σ_{max} is the maximum stress by pure elasticity, and σ_a is the elastic-plastic stress amplitude.

Using the cyclic stress-strain relation, i.e. the Ramberg-Osgood equation with parameter values given in Table 2, and the Molski and Glinka's equation, Eq. (19), the notch stress (amplitude) is determined to be 443 MPa with a plastic strain amplitude of 8.5E-5, and hence $\Delta\varepsilon_p$ = 1.7E-4. Using the TMW model, Eq. (6), the crack nucleation life is calculated to be 667,151 cycles. For the present case, the crack initiation size is defined as the distance from the notch root where the elastic stress is equal to 443 MPa, which is determined to be a_i = 0.13 mm from the stress analysis.

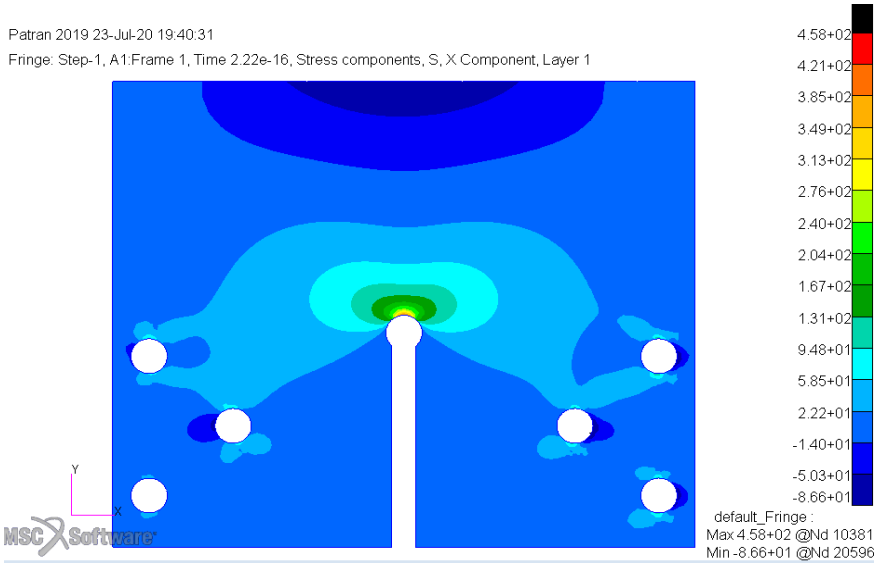

(a)

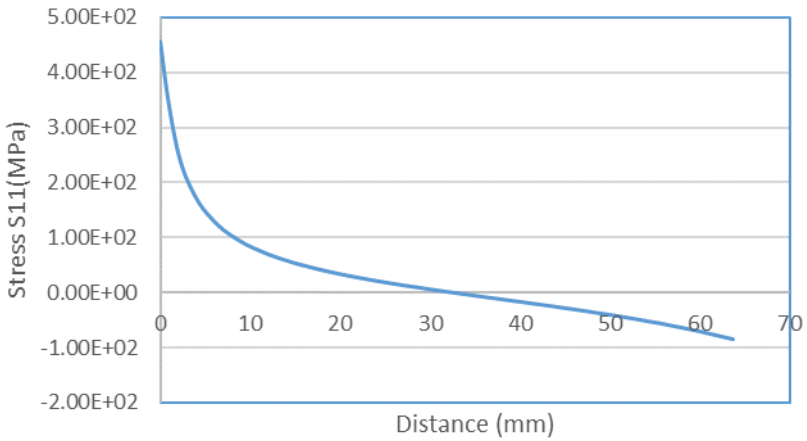

(b)

Figure 8. a) Stress contours in the key-hole specimen; b) stress distribution as function of distance from the notch root.

Fatigue crack growth simulation is conducted using FRANC3D with the crack growth rate as given by the Paris equation (eFatigue):

$$\frac{da}{dN} = 5.2 \times 10^{-9} \Delta K^{3.25} \ (\text{mm} \cdot \text{cycle}^{-1}) \qquad (21)$$

The simulated crack growth steps are shown in Figure 9 (Note K_I is plotted in the unit of MPa√mm, as computed in accordance with the FEM geometry model unit), and the calculated crack growth life from a_i = 0.13 mm to fracture toughness of 109 MPa is 78,519 cycles (Note that, only the positive load cycle is considered to drive crack growth). So, the total fatigue life is equal to 745,670 cycles. The experimentally observed crack initiation life was 605,000 cycles, and the remaining fatigue crack growth took 85,500 cycles, so the total experimental life was 690,500 cycles. The simulation (TMW model + FRANC3D) agrees with the experiment with 8% error.

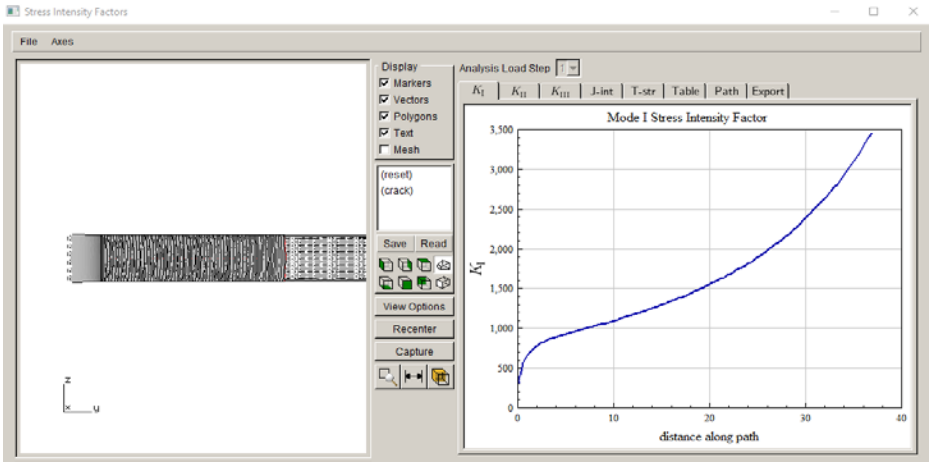

Figure 9. FRANC3D-simulated crack growth steps.

From this experiment and simulation analysis, a few points need to be further elaborated. First, the crack nucleated naturally at the key-hole notch root. The crack nucleation size is based on the length of plasticity distribution in the structure (specimen), as implied in the TMW model. Second, at this crack size (a_i = 0.13 mm), the maximum stress intensity factor is approximately 11 MPa√mm (~320/√1000, according to the FRANC3D results from Figure 9) due to the local stress concentration, which puts the crack well into the Paris regime, i.e., Stage II. Therefore, the TMW model and the Paris equation provides a reasonably good description for the continuous process of crack nucleation and growth to the failure of the specimen. Despite the sharp gradient of elastic stress near the notch root, as shown in Figure 8b, the simplification of uniform plastic deformation seems to work well in this situation, after the Neuber-Molski-Glinka correction. Of course, there are more situations that need to be addressed, especially with regards to how cracks would grow across the apparent "fatigue threshold", if naturally nucleated at smooth surfaces without local stress concentration. If the crack appears in Stage I after nucleation, it falls into the short-crack category. In this situation, continuously-distributed dislocation pile-up formulations can be used, even considering the anisotropic effects of the crack-residing grain(s) [5], but this is not further discussed in this paper due to the limited space. Given its importance, more case studies on continuous crack nucleation and growth simulations need to be included in the current structural integrity programs. Then, an important question follows, which is the standardization, validation and certification of HOLSIP analysis.

For structural integrity with natural growing cracks, understanding the probabilities of crack initiation is a critical issue, which is often (traditionally) addressed through testing of multiple samples to determine the probability of occurrence (size and location). An alternative approach is through microstructural fatigue simulation with prescribed grain size and orientation distribution as close as possible to the real material. The

physics underlying Eq. (6) can be easily incorporated into crystal plasticity analysis to identify the crack-nucleating grain(s). Work of this nature for smooth coupons is currently underway in the authors' laboratory. Of course, extensive simulation and physical testing are still needed to standardize the analytical procedures and data analysis, to cover a wide range of microstructural scenarios and possibly extremes, for validation and certification. The HOSIP simulation or "virtual testing" can migrate from coupon to component, following the same rules of physics, to address structural life prediction and uncertainty quantification in structural integrity management.

4.0 CONCLUSIONS

The issues regarding the holistic structural integrity process consisting of crack nucleation, stage I and stage II crack growth and final fracture are critically reviewed and discussed with the aim to establish a self-consistant methodology linking the life prediction analyses for the above stages to fullfil the requirements of integrated vehicle health management and prognosis. Several salient points are made in the following.

1. It has been shown that LCF crack nucleation life can be analytically predicted using the TMW model based on the applied plastic strain range, while knowing the material's elastic modulus, Poisson's ration, Burgers vector, surface energy and surface roughness, without resorting to fatigue testing. For structural applications, the cyclic plastic strain can be evaluated from the Ramberg-Osgood equation in terms of the cyclic parameters. Cyclic stress-strain curves can be established by step-increment cycling. However, as the traditional Ramberg-Osgood relation does not specify a threshold condition of plasticity, the fatigue endurance limit may still need to be determined by experiments, or use the stress-based TMW equation to extrapolate from known HCF data (theoretically, just one test condition).

2. The TMW model has been extended to variable amplitude fatigue crack nucleation, which is equivalent to the Palmgren-Miner rule, but determines the fatigue life in terms of the root mean square (RMS) of the loading spectrum.

3. Regarding crack growth, different treatments may be needed depending on whether the nucleated crack falls in Stage I or Stage II. Stage I crack lying on a particular slip system can be treated with the continuously distributed dislocation theory in a way similar to the TMW model, but considers the crack surface in a traction-free condition. Moving into Stage II or long crack regime, the Paris equation is applicable.

4. For continuous crack nucleation and growth in HOLSIP, the TMW model is shown to be successful to describe natural crack nucleation from a stress concentration region after Neuber/Molski-Glinka's correction for the local plastic strain. The subsequent Stage II crack growth can be described by the Paris law.

ACKNOWLEDGEMENT

The work is conducted under the Defence Technologies and Sustainment (DTS) program of NRC.

REFERENCES

[1] Wöhler A. (1867), "Wöhler's experiments on the strength of metals." Engineering, Vol. 4, pp. 160-161.

[2] Forsyth, P.J.E. (1963), "Fatigue damage and crack growth in aluminium alloys." Acta Metall., Vol. 11, pp. 703-715.

[3] Swenson, D. O. (1969), "Transition between stage I and stage II modes of fatigue crack growth, Journal of Applied Physics, Vol. 40, p. 3467, https://doi.org/10.1063/1.1658221.

[4] Komorowski, J.P. (2016), "From Science to Engineering Practice - Evolving a Structural Integrity Framework." ASTM Jo Dean Morrow Fatigue Lecture. ASTM E08 Executive Committee, May 3, 2016, San Antonio, TX, USA. http://www.astm.org/COMMIT/ASTM%202016%20Fatigue%20Lecture%20 Komorowski.pdf.

[5] Wu, X.J. (2019), Deformation and Life Evolution in Crystalline Materials—an Integrated Creep-Fatigue Theory, CRC Press, New York, NY.

[6] Yool, K., Sheehy, S. and Lenhardt, D. (2006), A Survey of Aircraft Structural-Life Management Programs in the U.S. Navy, the Canadian Forces, and the U.S. Air Force. RAND Corporation, Santa Monica, CA 90407-2138.

[7] Thompson, N., Wadsworth, N.J. and Louat, N. (1956), "The origin of fatigue fracture in copper." Phil. Mag., Vol. 1, pp. 113-126.

[8] Essmann, U., Gösele, U. and Mughrabi, H. (1981), "A model of extrusions and intrusions in fatigued metals I. Point-defect production and the growth of extrusions". Phil. Mag., Vol. 44, pp. 405–426.

[9] Ma, B.-T. and Laird, C. (1989), "Overview of fatigue behaviour in copper single crystals - II. Population, size, distribution and growth kinetics of stage i cracks for tests at constant strain amplitude". Acta Metall., Vol. 37, pp. 337-348.

[10] Mughrabi, H. (2009), "Cyclic slip irreversiblilities and the evolution of fatigue damage". Metall. Mater. Trans. A, Vol. 40A, pp. 1257-1279.

[11] Tanaka, K., and Mura, T. (1981), "A dislocation model for fatigue crack initiation." J. App. Mech., Vol. 48, pp. 97-103.

[12] Wu, X.J. (2018), "On Tanaka-Mura's fatigue crack nucleation model and validation." Fat. Fract. Eng. Mat. & Struct., Vol. 41 No. 4, pp. 894-899.

[13] Tyson, W.R. and Miller, W.A. (1977), "Surface free energies of solid metals: estimation from liquid surface tension measurements". Surface Science, Vol. 62, pp. 267-276.

[14] Wareing, J, H. and Vaughan, G. (1979), "Influence of surface finish on low-cycle fatigue characteristics of Type 316 stainless steel at 400°C". Metal Science, January, pp. 1-8.

[15] Mughrabi, H. and Höppel, H. W. (2010), "Cyclic deformation and fatigue properties of very fine-grained metals and alloys." Int. J. Fatigue, Vol. 32, pp. 1413-1427.

[16] Zhang, Z.F., Gu, H.C. and Tan, X.L. (1998), "Low-cycle fatigue behaviours of commercial-purity

titanium." Mater. Sci. & Eng. A, Vol. 252, pp. 85-92.

[17] Schmunk, R.E. and Korth, G.E. (1981), "Tensile and low-cycle fatigue measurements on cross-rolled tungsten." J Nuclear Mater, Vol. 103&104, pp. 943-948.

[18] Lerch, B.A. and Jayaraman, N. (1984), "A study of fatigue damage mechanisms in Waspaloy from 25 to 800 °C." Mater. Sci. & Eng., Vol. 66, pp. 151-166.

[19] Reuchet, J. and Remy, L. (1979), "High temperature fatigue behaviour of a cast cobalt base superalloy." Fat. Fract. Eng. Mater. Struct., Vol. 2, pp. 51-62.

[20] Coffin, L.F. (1954), "A study of the effects of cyclic thermal stresses on a ductile metal." Transactions of the American Society of Mechanical Engineers, Vol. 76, pp. 931-950.

[21] Manson, S.S. (1954), Behaviour of materials under conditions of thermal stresses. National Advisory Commission on Aeronautics Report 1170, Lewis Flight Propulsion Laboratory, Cleveland, OH.

[22] Basquin, O.H. (1910), "The exponential law of endurance tests." Proceedings of American Society for Testing and Materials, Vol. 10, pp. 625-630.

[23] Noroozi, A. H., Glinka, G. and Lambert, S. (2005), "A two parameter driving force for fatigue crack growth analysis." Int. J. Fatigue, Vol. 27, pp. 1277–1296.

[24] Socie, D.F. and Morrow, J. (1980), "Review of contempory approaches to fatigue damage analysis", in Burke. J.J. and Weiss, V. (Eds.), Risk and Failure Analysis for Improved Performance & Reliability, Plenum Press, New York.

[25] Li, S., Wu, X.J., Liu R., and Zhang, Z. (2021), "Full-range fatigue Life prediction of metallic materials for full-range fatigue using the Tanaka-Mura-Wu model", SAE MobilityRxivTM Preprint, August 7, 2021, https://doi.org/10.47953/SAE-PP-00164.

[26] Pålmgren, A. 1924. "The fatigue life of ball-bearings." Z. VDI, Vol. 68, pp. 339–341 [in German].

[27] Miner, M.A. 1945. "Cumulative damage in fatigue." J. Appl. Mech., Vol. 12, pp. A159–A164.

[28] Aid, A., Amrouche, A., Bouiadjra, B, (2011), "Fatigue life prediction under variable loading based on a new damage model." Materials & Selection, Vol. 32, pp. 183-191.

[29] Ritchie, R. O. and Lankford, J. (1986), "Small fatigue cracks: a statement of the problem and potential solutions." Materials Science and Engineering, Vol. 84, pp. 11-16.

[30] Lankford, J. (1977) "Initiation and early growth of fatigue cracks in high strength steels." Eng. Fract. Mech., Vol. 9, pp. 617–624.

[31] Hudak, S.J. (1981), "Small crack behavior and the prediction of fatigue life." J. Eng. Mater. Technol., Vol. 103, p. 26.

[32] Miller, K.J. (1982), "The short crack problem." Fatigue and Fracture Eng. Mater. Struct., Vol. 5, p. 223.

[33] Ritchie, R.O. and Suresh, S. (1983), "The fracture mechanics similitude concept: questions concerning its application to the behavior of short fatigue cracks," Mater. Sci. Eng., Vol. 57, p. L27.

[34] Lankford, J. (1985), "The influence of microstructure on the growth of small fatigue cracks", Fatigue Fract. Eng. Mater. Struct., Vol. 8, p. 161.

[35] Ritchie, R. O. and Lankford, J. (Eds.) (1986), Small Fatigue Cracks, Metallurgical Society of AIME, Warrendale, PA.

[36] Lankford, J., Davidson, D.L. Suresh, S. (Eds.) (1984), Fatigue Crack Threshold Concepts, Metallurgical Society of AIME, Warrendale, PA.

[37] ASTM E647-15e1, Standard Test Method for Measurement of Fatigue Crack Growth Rates, ASTM International, West Conshohocken, PA, 2015, www.astm.org.

[38] Newman, J.C., Jr., and Edward, P.R. (1988), "Short-crack growth behaviour in an aluminum alloy: an AGARD cooperative test programme". AGARD-R-732, NATO, Advisory Group for Aerospace Research and Development.

[39] Liao, M. (2009), "Probabilistic modeling of fatigue related microstructural parameters in aluminum alloys." Eng. Fract. Mech., Vol. 76, pp. 668–680.

[40] Liao, M. (2010), "Dislocation theory based short crack model and its application for aircraft aluminum alloys". Eng. Fract. Mech., Vol. 77, pp. 22–36.

[41] Tanaka, K. (1986), "Modeling of propagation and non-propagation of small fatigue cracks." In Ritchie, R. O. and Lankford, J. (Eds.), Small Fatigue Cracks, pp. 343-362, Metallurgical Society of AIME, Warrendale, PA.

[42] Suresh, S. and Ritchie, R.O. (1984), "Propagation of short fatigue cracks". Int. Metall. Rev., Vol. 29, p. 445.

[43] Gangloff, R.P. (1985), "Crack size effects on the chemical driving force for aqueous corrosion fatigue." Metall. Trans. A, Vol. 16A, pp. 953–969.

[44] Molent, L. and Dixon, B. (2019), "Airframe metal fatigue revisited," Int. J. Fatigue, Vol. 131: doi: 10.1016/j.ijfatigue.2019.105323.

[45] Sadananda, K., Babu, M. N., Vasudevan, A.K. (2019), "A Review of fatigue crack growth resistance in the short crack growth regime." Materials Science & Engineering A, Vol. 754, pp. 674–701.

[46] Bilby, B.A., Cottrell, A.H. and Swinden, K.H. (1963), "The spread of plastic yield from a notch." Proc. R. Soc. Lond. A, Vol. 272, pp. 304-314.

[47] Tanaka, K. and Nakai, Y. (1983), "Propagation and non-propagation of short fatigue cracks at a sharp notch." Fatigue of Engineering Materials and Structures, Vol. 6, pp. 315-327.

[48] Tanaka, K., Akiniwa, Y. and Wei, R.P. (1986), "Modelling of small fatigue crack growth interacting with grain boundary." Eng. Fract. Mech., Vol. 24, pp. 803-819.

[49] Navarro, A and de los Rios, E.R. (1988), "Short and long fatigue crack growth: a unified model." Phil. Mag. A, Vol. 57, pp. 15-36.

[50] Wu, X.J. (2019), "A Fatigue crack nucleation model for anisotropic materials." Fatigue Fract Eng Mater Struct., Vol. 42, pp. 387-393.

[51] Stroh, A. N. (1958), “Dislocations and cracks in anisotropic elasticity.” Phil. Mag., Vol. 3, pp. 625-646.

[52] Ting T.C.T. (1996), Anisotropic Elasticity: Theory and Applications. Oxford University Press, Oxford.

[53] Marx, M., Vehoff, H., Schäf, W. and Welsch, M. (2006), “The mechanisms of the interaction of microcracks with grain boundaries: in-situ investigations in sem by fib, ebsd and electron channelling contrast.” In: Proc. 16th European Conference on Fatigue (CD-ROM), July 4-7, 2006, Alexandropoulis, Greece.

[54] Paris, P.C. and Erdogan, F. 1963. “A critical analysis of crack propagation laws.” Journal of Basic Engineering, Vol. 85, pp. 528-34.

[55] Wu, X.J., Koul, A.K. and Krausz, A.S. (1993), “A transgranular fatigue crack growth model based on restricted slip reversibility.” Metall. Trans. A, Vol. 24 A, pp. 1373-1380.

[56] Speidel, M.O. (1973), “Modulus of elasticity and fatigue crack growth.” In: High Temperature Materials in Gas Turbine: Proceedings of the Symposium on High Temperature Materials in Gas Turbines, pp. 212-221, Brown, Boveri & Company Limited, Baden, Switzerland.

[57] Wu, X.J., Wallace, W., Raizenne, M.D. and Koul, A.K. (1994), “The orientation dependence of fatigue crack growth rate in 8090 aluminum-lithium plate”. Metall. Trans. A, Vol. 25A, pp. 575-588.

[58] Elber, W. (1970), “Fatigue crack closure under cyclic tension.” Eng. Fract. Mech., Vol. 2, pp. 37-45.

[59] Elber, W. (1971), “The significance of fatigue crack closure.” In: Damage Tolerance in Aircraft Structures, ASTM STP 486, pp. 230-42, American Society for Testing and Materials. Philadelphia, PA.

[60] Suresh, S. and Ritchie, R.O. (1984), “Near-threshold fatigue crack propagation: a perspective on the role of crack closure.” In Davidson, D. and Suresh, S. (Eds.), Fatigue Crack Growth Threshold Concepts, pp. 227-261. The metallurgical Society of AIME, Warrendale, PA.

[61] McEvily, A.J. and Minakawa, K. (1984), “Crack closure and the growth of short and long fatigue cracks,” Scrpt. Metall., Vol. 18, pp. 71–76.

[62] Newman, J.C. and Elber, W. (Eds.) (1988), Mechanics of Fatigue Crack Closure, ASTM STP 982, Philadelphia.

[63] Kitagawa, H. and Tanaka, T. (Eds.) (1990), Fatigue’ 90: Proceedings of the Fourth International Conference on Fatigue and Fatigue Thresholds, Materials and Component Engineering, Birmingham, UK.

[64] Forman, R. G., Kearney, V. E., Engle, R. M. (1967), "Numerical analysis of crack propagation in cyclic-loaded structures". Journal of Basic Engineering. Vol. 89 (3), pp. 459–463.

[65] McEvily, A. J. and Groeger, J. (1978), "On the threshold for fatigue crack growth", Advances in Research on the Strength and Fracture of Materials, Elsevier, pp. 1293–1298.

[66] Walker, K. (1970), "The effect of stress ratio during crack propagation and fatigue for 2024-t3 and 7075-T6 aluminum", Effects of Environment and Complex Load History on Fatigue Life, ASTM International, pp. 1–14

[67] Allen, R. J., Booth, G. S., Jutla, T. (1988), "A review of fatigue crack growth characterisation by linear

elastic fracture mechanics (LEFM). Part II – advisory documents and applications within national standards". Fatigue & Fracture of Engineering Materials and Structures, Vol. 11 (2), pp. 71–108.

[68] Forman, R. G., Shivakumar, V., Cardinal, J. W., Williams, L. C., McKeighan, P.C. (2005), "Fatigue Crack Growth Database for Damage Tolerance Analysis." FAA.

[69] Wu, X.J. (1995), “An energy approach to crack closure. Int. J. Fract., Vol. 73, pp. 263-272.

[70] Wu, X. J., Wallace, W. and Koul, A.K. (1995), “A new approach to fatigue threshold.” Fat. & Fract. Eng. Struct. & Mat., Vol. 18, pp. 833-845.

[71] Wu, X.J., Wallace, W., Koul, A.K. and Raizenne, M.D. (1995), “Near-threshold fatigue crack growth in 8090 al-li alloy.” Metall. Trans. A, Vol. 26A, pp. 2973-2982.

[72] Molski, K. and Glinka, G. (1981), “A method of elastic-plastic stress and strain calculation at a notch root.” Materials Science and Engineering, Vol. 50, pp. 93 – 100.